Supporting Information

for

Co oxide nanostructures for electrocatalytic water-oxidation: Effect of dimensionality and related properties

S. Gupta[a]*, A. Yadav[b], S. Bhartiya[c], M. K. Singh[c], A. Miotello[d], A. Sarkar[a], N. Patel[b]

[a]Department of Chemical Engineering, Indian Institute of Technology Bombay, Powai, Mumbai-400076, India.

[b]Department of Physics, University of Mumbai, Santacruz (E), Mumbai 400 098, India.

[c]Laser Material Section, Raja Ramanna Centre for Advanced Technology, Indore, India.

[d]Dipartimento di Fisica, Università degli Studi di Trento, I-38123 Povo, Trento, Italy.

Additional Experimental Details:

Chemicals and Materials:

Cobalt nitrate hexahydrate [$Co(NO_3)_2.6H_2O$, 99%] (SDFCL), Cobalt acetate [$C_4H_6CoO_4$, 99.9%] (Sigma-Aldrich), Urea [$Co(NH_2)_2$, 98%] (SDFCL) and Sodium Fluoride [NaF, 98.5%] (Merck) were used for synthesizing the catalysts. Potassium hydroxide [KOH, 98%] (Merck) was used to prepare the electrolyte solution. Deionized water (Millipore) was used for all practical purposes.

Photo-Fenton degradation reaction:

The photocatalytic performance of the Co oxide nanostructures was evaluated by degradation of methylene blue (MB) dye under photon irradiation. A borosilicate photochemical reactor (250 mL) was used along with a 150 W collimated Xenon arc lamp (Hamamatsu) in a top-down assembly. The photo-reactor was placed at a fixed distance of 47cm from the Xe source. 5 mg of each Co oxide sample was added to 50 mL of 10 ppm MB dye solution and 1 mL of hydrogen peroxide (H_2O_2, 30%) which acts as the oxidizing agent for photo-fenton reaction. Prior to beginning the degradation test, the entire mixture is kept in the dark and stirred for about 30 min so that the adsorption/desorption equilibrium is established between the catalyst surface and the dye solution. Once the equilibrium is established, the dye-catalyst solution is irradiated with Xe arc lamp to study the degradation of dye. With light irradiation, at regular intervals of 10 minutes, 3 mL of reaction solution was withdrawn and an absorption spectra was recorded using a UV-Vis spectrophotometer (Implen Nano Photometer). The change in concentration of MB dye is analyzed by observing the decrement in absorption wavelength of 665 nm, which is characteristic to MB dye. All the experiments were performed at room temperature and were repeated at least 3 times to confirm the reproducibility of the results.

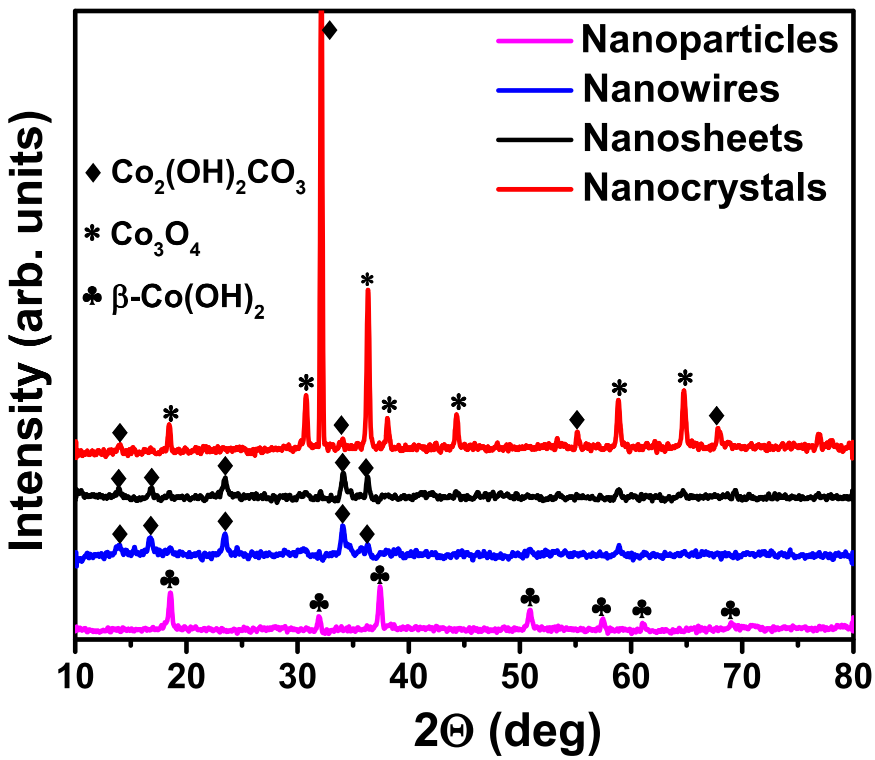

Fig. S1: Powder X-ray diffraction spectra for as prepared Co hydroxide nanoparticles, nanowires, nanosheets and nanocrystals.

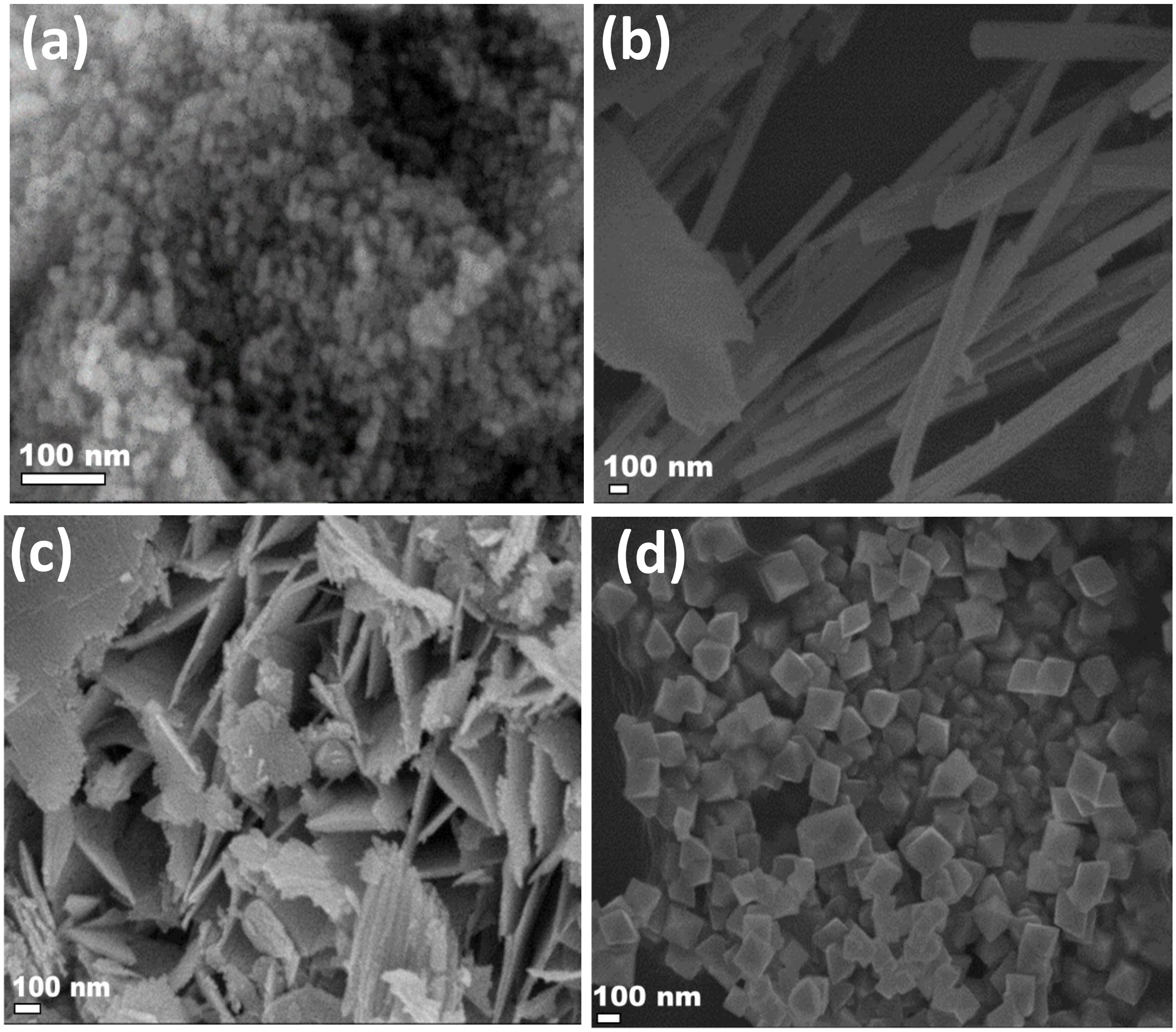

Fig. S2: SEM images of annealed Co_3O_4 **(a) nanoparticles, (b) nanowires, (c) nanosheets and (d) nanocrystals.**

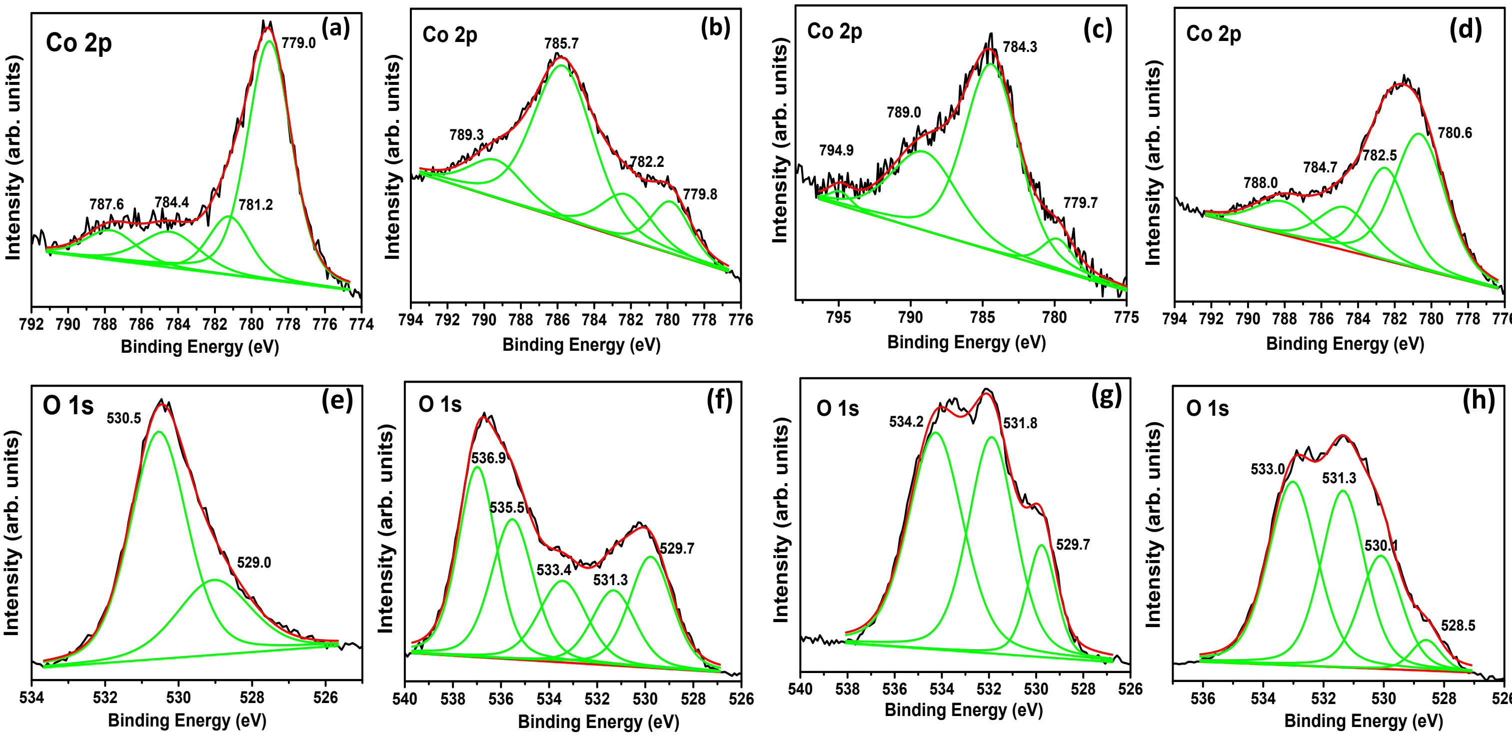

Fig. S3. X-ray photo-electron spectra showing **Co 2p$_{3/2}$** and **O 1s** states for as prepared Co oxide **(a, e) nanoparticles, (b, f) nanowires, (c, g) nanosheets** and **(d, h) nanocrystals, respectively**.

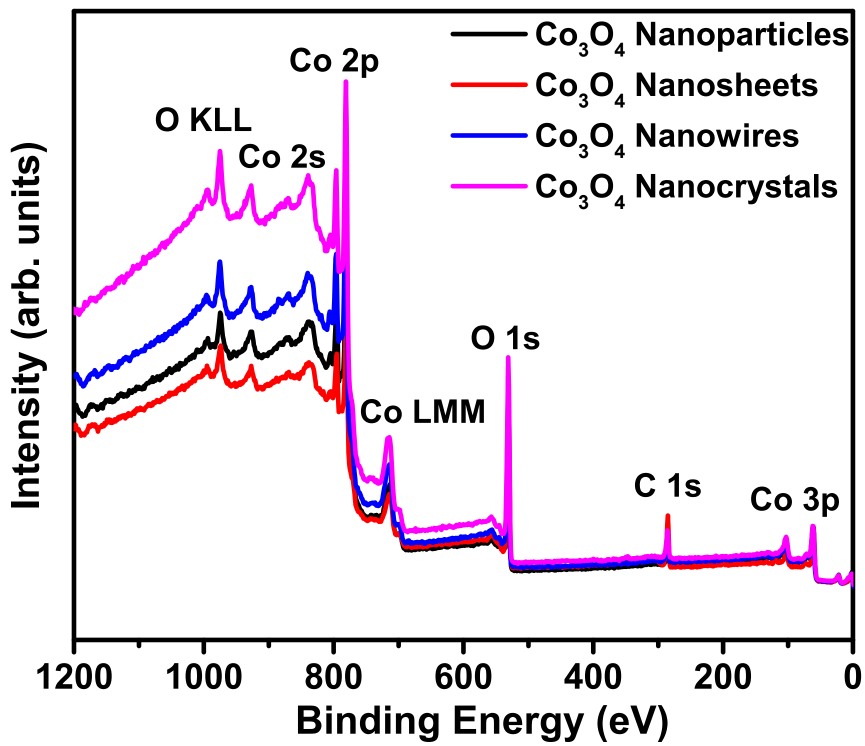

Fig. S4. XPS survey spectra of Co_3O_4 nanostructures revealing presence of Co, O and C only, with no other impurities.

Sample	At% Composition from XPS		At% Composition from EDAX	
	Co	O	Co	O
Co_3O_4 Nanoparticles	44.37	55.63	41.37	58.63
Co_3O_4 Nanowires	45.44	54.56	46.88	53.12
Co_3O_4 Nanosheets	34.30	65.70	36.89	63.11
Co_3O_4 Nanocrystals	39.98	60.02	45.02	54.98

Table S1: Table showing percentage atomic composition of Co and O in annealed Co_3O_4 nanostructures obtained from XPS and EDAX.

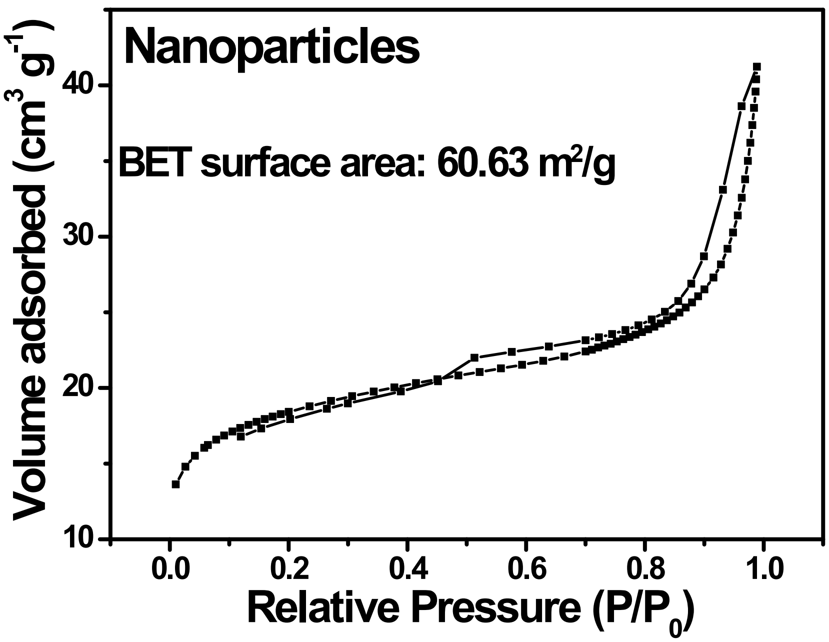

Fig. S5: N_2 adsorption-desorption isotherms obtained from BET measurements for **$Co(OH)_2$ NPs**, showing H1 type of hysteresis loop belonging to Type IV isotherm.

Catalyst	BET Surface Area (m^2/g)	Average pore diameter (nm)	Pore Volume (cm^3/g)
Co_3O_4 Nanoparticles	23.2	3.0	0.0082
Co_3O_4 Nanowires	22.0	15.0	0.0768
Co_3O_4 Nanosheets	24.1	4.5	0.0191
Co_3O_4 Nanocrystals	15.6	3.9	0.0040

Table S2: Table showing physico-chemical properties of Co_3O_4 nanostructures obtained by BET measurement.

Catalyst	Electrolyte	Overpotential (mV vs RHE) to achieve		Tafel plot (mV/dec)	Reference
		10 mA/cm^2	100 mA/cm^2		
Co_3O_4 NPs	1 M KOH	392	430	44	This work
Co_3O_4 NWs	1 M KOH	392	447	53	This work
Co_3O_4 NSs	1 M KOH	394	456	52	This work
Co_3O_4 NCs	1 M KOH	405	480	58	This work
Co_3O_4@ carbon paper	1 M KOH	310	--	69	[1]
Co_3O_4 nanocubes@ NGraphene	1 M KOH	280	--	69	[2]
Co_3O_4 Carbon porous Nano Arrays	0.1 M KOH	290	--	70	[3]
Sn doped Co_3O_4	0.1 M KOH	354	--	85	[4]
Ni doped Co_3O_4	0.1 M KOH	360	--	91	[4]
Fe doped Co_3O_4	0.1 M KOH	370	--	87	[4]
$Co_3O_4/NiCo_2O_4$	1 M KOH	340		88	[5]
Mesoporous Co_3O_4 nanoflakes	1 M KOH	380	--	48	[6]
Commercial Co_3O_4	1 M KOH	451	--	59	[6]
$NiCo_2O_4$	1 M KOH	330	--	60	[7]
$CoNiO_x$@rGO	0.1 M KOH	320	--	45	[8]
Co_3O_4@rGO	0.1 M KOH	370	--	64	[8]
$CoNiO_x$	0.1 M KOH	367	--	69	[8]
Co_3O_4@N-porous carbon	0.1 M KOH	390	--	72	[9]
Reduced Co_3O_4	1 M KOH	340	--	47	[10]
Mesoporous Co_3O_4	0.1 M KOH	411	--	60-70	[11]
Co_3O_4 thin film	1 M NaOH	377	--	58	[12]
Ir/C	0.1 M KOH	370	--	91	[9]
RuO_2	1 M KOH	370	457	88	This work

Table S3: Comparison of electrochemical parameters for OER between Co_3O_4 nanostructures with other reports on Co_3O_4 based catalysts in alkaline medium.

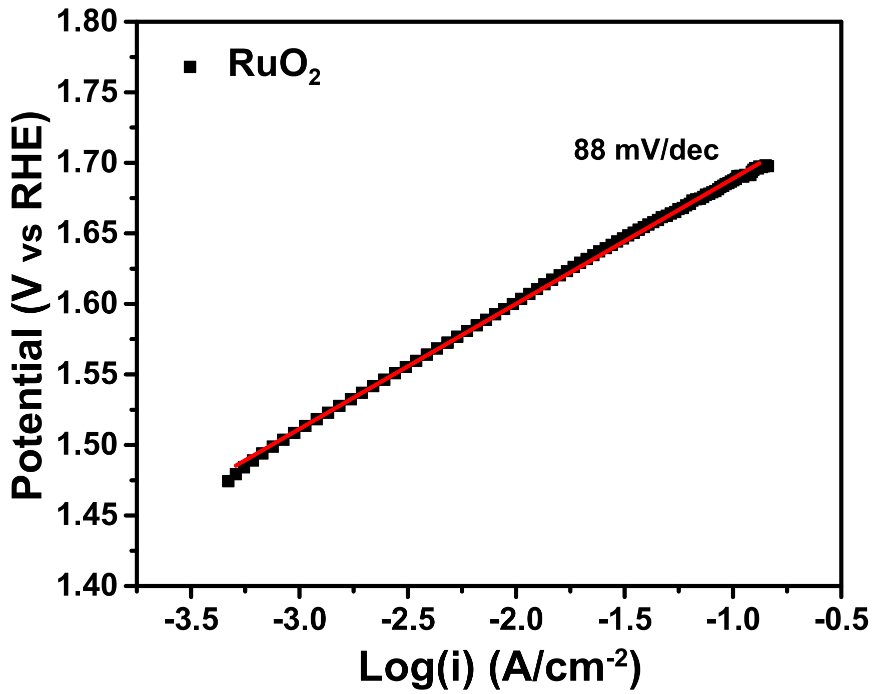

Fig. S6: Tafel plot for commercial RuO_2 catalyst, yielding a Tafel slope value of 88 mV/dec.

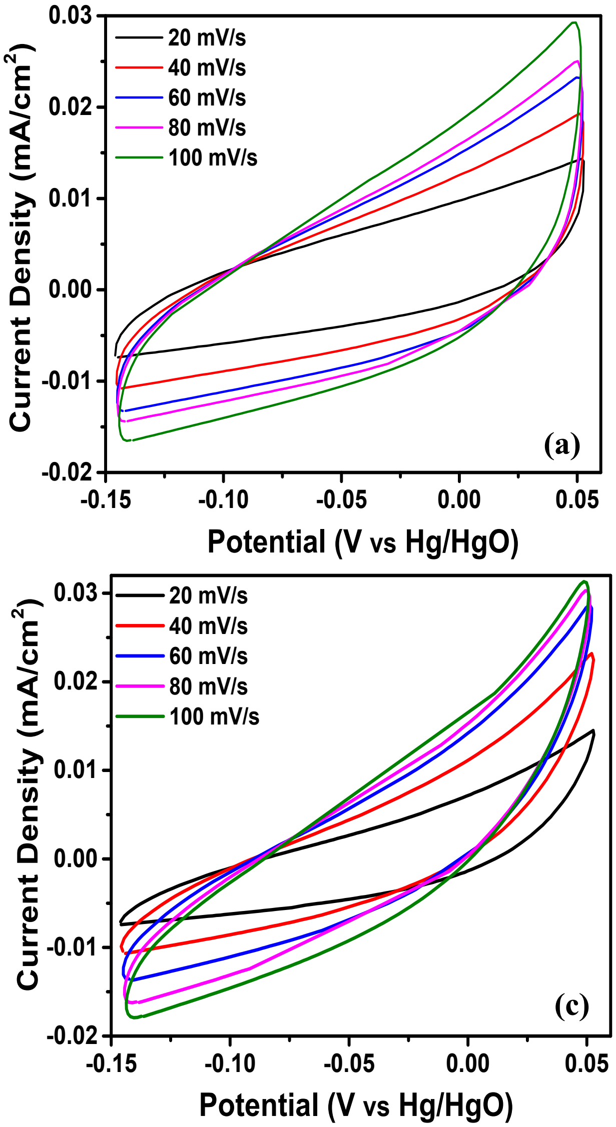

Fig. S7: CV curves at different scan rates for Co_3O_4 **(a) nanoparticles, (b) nanowires, (c) nanosheets and (d) nanocrystals** in Ar saturated 1 M KOH solution to determine the double layer capacitance (C_{DL}).

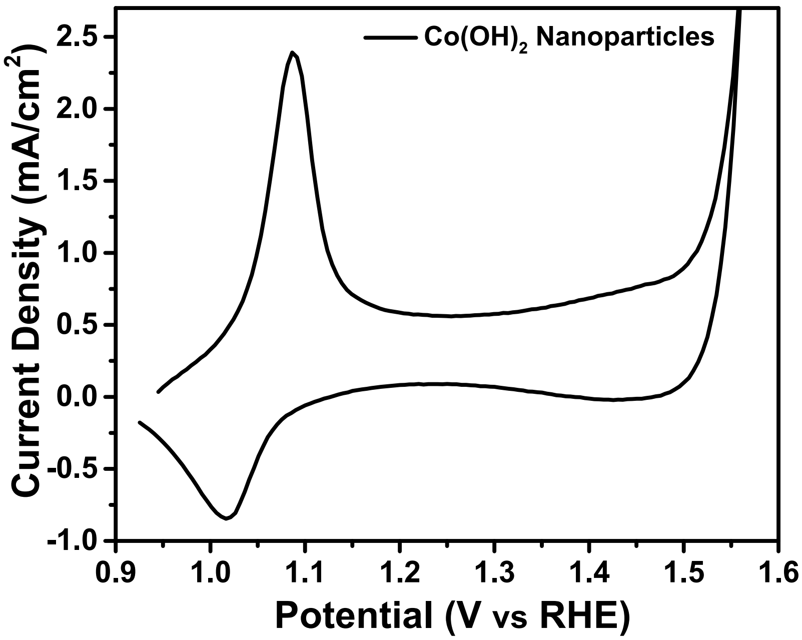

Fig. S8: CV curve for $Co(OH)_2$ nanoparticles in Ar saturated 1 M KOH solution at a scan rate of 5 mV/s.

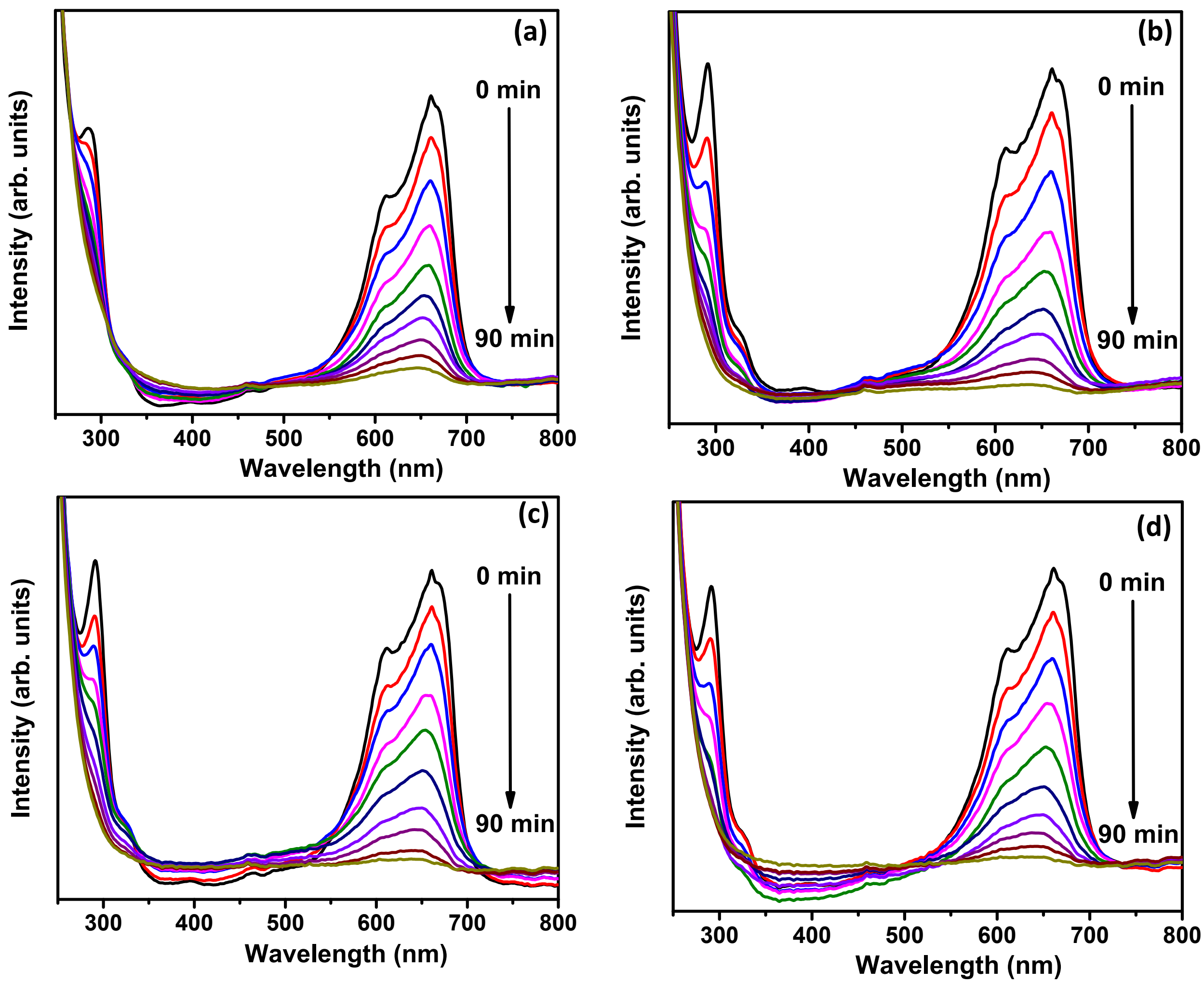

Fig. S9: Decrease in characteristic UV-Vis absorption peak of MB dye with time under Xe lamp illumination in presence of Co_3O_4 **(a) nanoparticles, (b) nanowires, (c) nanosheets and (d) nanocrystals,** via photo-Fenton reaction.

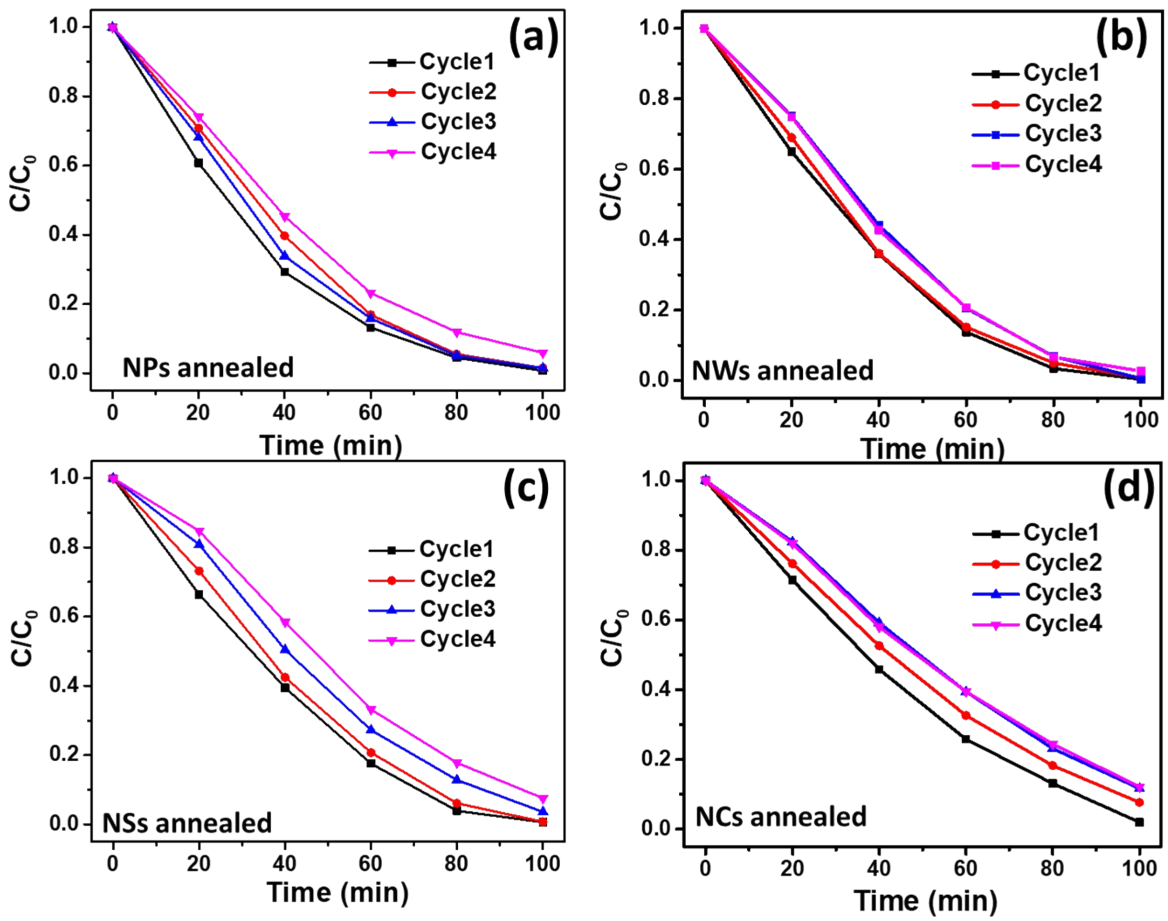

Fig. S10. Recycling test for degradation of MB dye via photo-Fenton reaction for Co_3O_4 **(a) nanoparticles, (b) nanowires, (c) nanosheets and (d) nanocrystals.**

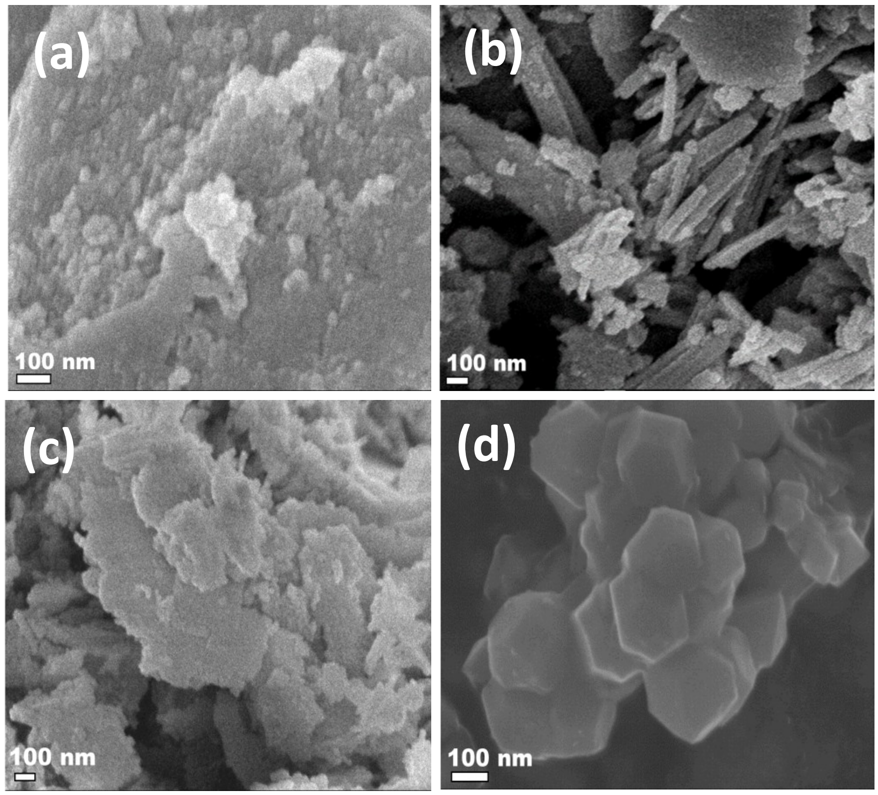

Fig. S11: SEM images of Co_3O_4 **(a) nanoparticles, (b) nanowires, (c) nanosheets and (d) nanocrystals,** after 4 cycles of photo-Fenton reaction.

References:

1 X. Yang, H. Li, A.-Y. Lu, S. Min, Z. Idriss, M. N. Hedhili, K.-W. Huang, H. Idriss and L.-J. Li, *Nano Energy*, 2016, **25**, 42–50.

2 S. K. Singh, V. M. Dhavale and S. Kurungot, *ACS Appl. Mater. Interfaces*, 2014, **7**, 442–451.

3 T. Y. Ma, S. Dai, M. Jaroniec and S. Z. Qiao, *J. Am. Chem. Soc.*, 2014, **136**, 13925–13931.

4 N.-I. Kim, Y. J. Sa, S.-H. Cho, I. So, K. Kwon, S. H. Joo and J.-Y. Park, *J. Electrochem. Soc.*, 2016, **163**, F3020–F3028.

5 H. Shi and G. Zhao, *J. Phys. Chem. C*, 2014, **118**, 25939–25946.

6 S. Chen, Y. Zhao, B. Sun, Z. Ao, X. Xie, Y. Wei and G. Wang, *ACS Appl. Mater. Interfaces*, 2015, **7**, 3306–3313.

7 Z. Peng, D. Jia, A. M. Al-Enizi, A. A. Elzatahry and G. Zheng, *Adv. Energy Mater.*

8 P. Li and H. C. Zeng, *Adv. Funct. Mater.*

9 Y. Hou, J. Li, Z. Wen, S. Cui, C. Yuan and J. Chen, *Nano Energy*, 2015, **12**, 1–8.

10 Y.-R. Liu, G.-Q. Han, X. Li, B. Dong, X. Shang, W.-H. Hu, Y.-M. Chai, Y.-Q. Liu and C.-G. Liu, *Int. J. Hydrogen Energy*, 2016, **41**, 12976–12982.

11 Y. J. Sa, K. Kwon, J. Y. Cheon, F. Kleitz and S. H. Joo, *J. Mater. Chem. A*, 2013, **1**, 9992–10001.

12 H. S. Jeon, M. S. Jee, H. Kim, S. J. Ahn, Y. J. Hwang and B. K. Min, *ACS Appl. Mater. Interfaces*,

2015, **7**, 24550–24555.